A levelized cost of energy approach to select and optimise emerging PV technologies: The relative impact of degradation, cost and initial efficiency

*Balder A. Nieto-Díaz,[1] Andrew F. Crossland,[2] Christopher Groves[1]**

[1]Department of Engineering, Durham University, South Road, Durham, DH1 3LE, United Kingdom

[2]Durham Energy Institute, Durham University, South Road, Durham, DH1 3LE, United Kingdom

[*]Correspondence: chris.groves@durham.ac.uk

Abstract

A model of levelized cost of energy (LCOE) is presented which accounts for the significant 'burn-in' losses common in photovoltaic (PV) devices with organic (OPV) and perovskite (PVK) absorber layers. This model is used to quantify the relative importance of burn-in, module cost and initial efficiency for a realistic grid-scale PV installation situated in Fiji. The effectiveness of improvements in PV technology in reducing LCOE is shown to depend critically upon the current status of the technology. Predictions of LCOE for specific state-of-the-art OPV and PVK devices sourced from the literature are presented, some of which are shown to have potential to compete at the grid scale. However, devices with state-of-the-art initial efficiencies are not necessarily those with state-of-the-art LCOE, emphasizing the need to characterize lifetime energy yield and for an LCOE approach to select the most promising candidate technologies.

Keywords

Levelized cost of energy, Perovskite photovoltaics, Organic photovoltaics, techno-economic modelling, degradation.

Highlights

- A levelized cost of energy (LCOE) for emerging photovoltaics (PV) is developed.
- Typical degradation profile of Perovskite and Organic PV is taken into account.
- Optimal strategies to improve LCOE depend upon present status of PV technology.
- LCOE is calculated for literature state-of-the-art Perovskite and Organic PV cells.
- Emerging PV have potential to compete with established Silicon PV LCOE.

Abbreviations:

LCOE	levelized cost of energy
PV	photovoltaic
OPV	organic photovoltaic
PVK	perovskite
Si	silicon
PCE	power conversion efficiency
B	burn-in
D	degradation rate
$\mathbf{PCE_i}$	initial efficiency
$\mathbf{PCE_B}$	post burn-in efficiency
NPV	net present value
EFL	Energy Fiji Limited
Wp	watt peak
kWh	kilowatt hour
ISOS	International summit on OPV stability
T_{S80}	stabilized lifetime
ETL	electron-transporting layer

1. Introduction

Emerging Photovoltaic (PV) devices based on perovskite and organic absorber layers have the potential to be a disruptive energy generation technology due to their low-cost manufacture [1, 2] and rapidly improving power conversion efficiency (PCE). Whether emerging PV will deliver on this promise at the grid scale depends to a large extent on the cost of energy it can provide. The established metric by which energy generation technologies are compared is the Levelized Cost of Energy (LCOE), which accounts for the accumulated energy and associated costs over the lifetime of a project. Herein lies a challenge for emerging PV, as energy yield degrades more rapidly than established silicon PV modules that are often warrantied to lose no more than 0.7% of their yield each year of their 25-year lifespan on average [3]. It is not clear how the competing impacts of cost, efficiency and degradation impact the current competitiveness of emerging PV, nor how one quantitatively directs technology development to meet future needs.

In this paper, we address these challenges by presenting a new model of LCOE that quantifies the impact of rapid degradation at the start of a module's life (burn-in) that is characteristic of emerging PV technologies. This model was used to quantify the relative impacts of realistic degradation, initial efficiency and module cost upon LCOE. Further, the competitiveness of specific, state-of-the-art perovskite PV (PVK) and organic PV (OPV) reported in the literature are assessed for a realistic grid-scale PV installation in Fiji. It is shown that the approach one would take to optimize LCOE depends critically upon the current status of the technology, i.e. the module cost, initial

PCE, and following degradation. Further, it is found that ‘champion’ initial PCE devices are not necessarily those with ‘champion’ LCOE due to the significant impact of largely uncorrelated degradation within literature devices, underlining the importance of characterizing lifetime energy yield in candidate emerging PV devices. Ultimately, the model predicts that PVK and OPV devices have the potential to compete in wholesale electricity markets, but that the multivariate dependence of LCOE on cost, initial performance and degradation must be considered during research and consequent technology development.

2. Methodology

LCOE models are an increasingly popular tool to highlight the commercial benefits of emerging PV devices as well as highlighting remaining challenges. For example, several LCOE studies have taken bottom-up approaches to evaluate the impact of cost of materials (e.g. active layer) and manufacturing processes at lab, upscaling and industry levels, revealing that potential bottlenecks to low-cost OPV production lie in the cost of raw materials and not in processing costs [4-6]. Other studies have incorporated a Monte Carlo approach to determine a range of costs for emerging PV devices, whilst also highlighting the importance of efficiency, lifetime and other parameters by a sensitivity analysis [7, 8]. Furthermore, LCOE models have also shown the benefit to panel replacement when module performance increases rapidly due to advancing technology [9]. However, to the best of our knowledge, LCOE models of emerging PV have assumed degradation akin to technologically mature Silicon, rather than that which is characteristic of emerging PV. Elsewhere, works mainly focusing on mature PV technologies have shown the important impacts of degradation on LCOE [10, 11], however, these models were not designed to capture the complex degradation behaviour of emerging PV. Our focus in this paper is to develop a model which is based upon degradation characteristics reported in emerging PV devices for the first time. This enables us to provide insights specific to emerging PV devices by allowing the identification of development strategies and comparison with established, low degradation Si PV technology.

2.1 Establishing range of degradation behavior in emerging PV

To ensure that our model was able to accurately model the degradation behavior that is characteristic of emerging PV, we first performed a literature review of degradation behavior of PVK and OPV devices. The search engine Web of Science was used to perform a topic search for the terms ‘lifetime,’ ‘degradation’, ‘burn-in,’ ‘photovoltaic,’ ‘solar cell,’ and either ‘organic’ or ‘OPV’, or ‘perovskite’ on 8th Oct 2020, in the date range Jan 2013 to Jun 2020, returning 134 papers. To ensure we captured the state of the art, an additional topic search in which the terms ‘stable’ or ‘stability’ replaced lifetime related terms (lifetime or degradation or burn-in) was performed on 27th Jan 2021, with an extended date range from Jan 2013 to Dec 2020. The 100 most cited papers prior to 2019, and 2020 papers with more than 15 cites (65 papers) were considered. Each of the 299 papers returned by the searches were examined and information related to degradation profile, device structure and measurement conditions was noted. Only those papers which reported degradation behavior in sufficient detail are included in the following analysis. Table A1 of Appendix A summarizes the information obtained for the 38 OPV [9, 12-33] and 31 PVK [34-52] datasets revealed by the search, including materials used, structure, degradation and measurement conditions. These data were grouped into the following broad categories according to the measurement conditions:

- Light-soaking. Experiments which involved continuous illumination at or close to AM1.5G simulated sunlight with 1,000 W/m^2 intensity. The devices were either encapsulated in some manner (e.g. epoxy glued coverslips) or were tested in an atmosphere with reduced water vapor and oxygen content.
- Light-soaking without encapsulation. As light-soaking but without encapsulation and an ambient atmosphere similar to typical indoor conditions.
- Thermal aging: As light-soaking, but at elevated temperature of 85 °C.
- High-temperature storage: Devices were stored in the dark at elevated temperatures of 65/85 °C.
- Outdoor testing. Devices tested outdoors with either encapsulation or ambient atmosphere with reduced water vapor and oxygen content.

To mitigate the impact of differing measurement protocols, only those devices aged using light-soaking conditions were considered in the following analysis. This reduced dataset comprised 29 OPV and 26 PVK devices. We note that while outdoor measurement protocols are the closest to real-world conditions, there are too few measurements reported at time of writing to enable comparison between candidate emerging PV technologies. Thus, we select the light-soaking category as there is a wide range of reported device and materials data, and the measurements allow for the possibility of photo-oxidation of active materials.

A characteristic degradation profile that describes these data is shown in **Figure 1**A. This degradation profile comprises a rapid period of initial degradation, commonly known as 'burn-in,' followed by a slower but sustained period of linear degradation [53]. Burn-in may be caused by morphological changes in the blended materials of the active layer of emerging PV devices when exposed to light or heat [54, 55], as well as by the interfacial resistance between the electron-transporting layer (ETL) and the photoactive layer [20]. On the other hand, linear degradation is mainly caused by the ingress of water and oxygen to the device, which under illumination can react with the organic layers, resulting in photo-bleaching or minimal light-absorption ability [53]. We take a moment to comment on differing early-time degradation behaviors to those highlighted in the literature review. It has been shown that some PVK devices show partial burn-in recovery in the dark [56], although it is not clear to what extent this recovery would manifest itself in real-world conditions, and as such, is not included here. However, we note that the methodology presented here can calculate LCOE for degradation profiles with arbitrary time resolution, as would be needed to account for such effects. To first order, we expect burn-in recovery to be accounted for by a lower effective burn-in than measured under continuous illumination. About a quarter of devices (15) exhibited no burn-in, in which case, their degradation profile can be described by linear degradation only. While it is not expected that all emerging PV devices will be well-described by the parameterization shown in Figure 1A, all 55 datasets can be parameterized with this schema. Section 2.2 (Model development) discusses in more detail how the LCOE model can be modified to account for arbitrary degradation profiles as required. Returning to the data, it is shown that 'burn-in' occurs over a period, τ_B that is typically of the order of hundreds of hours in full sun [53]. We define the initial and post burn-in efficiencies are referred to as PCE_i and PCE_B respectively, with burn-in loss, B, being defined as the percentage loss in efficiency during the burn-in period (e.g. if PCE_i = 10% and PCE_B = 8%, B = 20%). PCE_i (%) and B (%) values were taken directly as specified in the papers. The linear degradation following burn-in is parameterized by a degradation rate, D, which is defined as the fractional percentage loss of post-burn in efficiency per year of operation.

The linear degradation rate, D (%/year) was calculated by dividing the difference between absolute post burn-in efficiency (PCE_b) and efficiency at the end of the test (PCE_{end}) by the intervening time period, though in some cases, the extrapolated lifetime reported in the paper (often the estimated time for post burn-in efficiency to drop by 20%) was used to calculate D instead. For the purpose of later LCOE calculations, it was necessary to interpret the time under constant illumination in a laboratory setting to a degradation rate per year, D (%/year) which reflects the diurnal and seasonal variation in sunlight in the project location [53]. In this calculation, it was assumed each day has 5.5 hours of direct full sunlight (equating to ~2,000 hours per year [19]) which was chosen to be similar to the 1,889 annual peak solar hours for the chosen installation location [57]. Further, we assumed that degradation only occurs during the hours of full sun, as it has been shown that the rate of aging in the dark is substantially lower in comparison [58]. The degradation rate was not calculated for those papers which did not provide sufficient information about the test lifetime.

The values of PCE_i, B and D for emerging PV devices aged under light-soaking conditions only are plotted against one another in Figure 1B-D. It is apparent that PCE_i

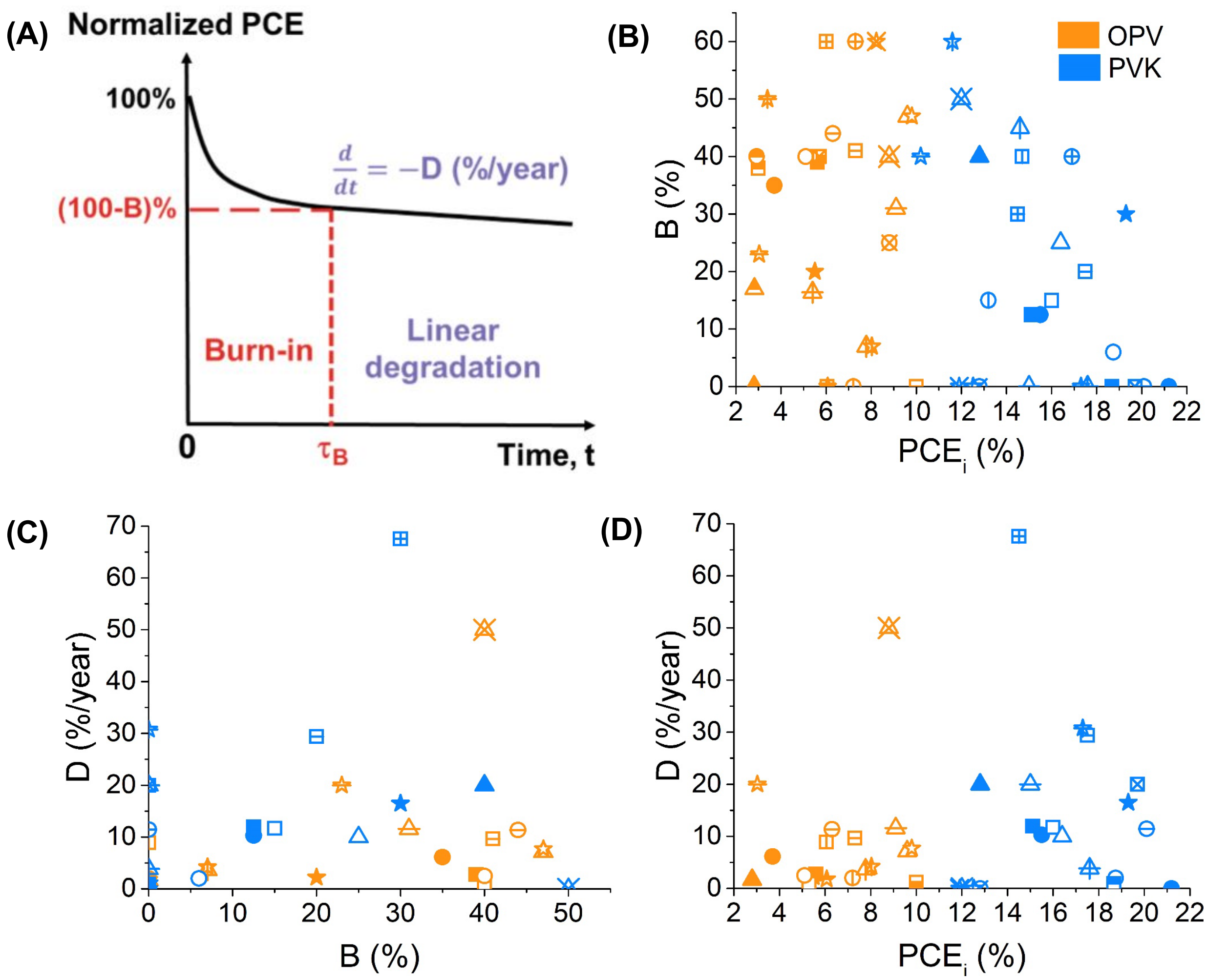

Figure 1. Emerging PV Characteristic Parameters from literature review

(A) Schematic representation of the typical evolution of PCE in OPV and PVK devices. Plots of (B) Burn-in vs PCE, (C) degradation rate vs burn-in, and (D) degradation rate vs PCE reported in the literature for PVK (blue) and OPV (orange) devices. Each symbol represents a unique device, the materials and architecture for which is listed in table A8 of the supplementary information.

for OPVs is typically lower than PVK devices, but otherwise there appears to be little correlation amongst the datasets. To further clarify relationships between these data, the Pearson correlation coefficient was calculated for each pair of characteristics in the light-soaking category, as shown in **Table 1**. Degradation rates of 30%/year or more were omitted from the analysis as unrepresentative outliers. The correlation coefficients for OPVs were close to zero (0.04, -0.08, 0.31), indicating weak correlation between PCE_i, B and D. By comparison, PVKs display a stronger negative correlation between PCE_i and burn-in (-0.46). This suggests that the factors determining lifetime evolution of PCE in OPVs are to some extent orthogonal, whilst in PVKs, there is some correlation between initial performance and degradation as discussed elsewhere [59-61]. It is noted that the certified record efficiencies for lab-scale PVK and OPV devices [62] are far in excess of the highest reported initial efficiency of lab-scale devices that have undergone degradation studies shown in Figure 1. This gap in performance is equivalent to a time-lag of ~7 years for OPV devices and ~3 years for PVK devices, and it emphasizes the need for standardized degradation tests [63, 64] on the latest PV materials and architectures.

Table 1. Pearson coefficients and average characteristics of Figure 1 devices

	Pearson coefficients			**Device characteristics**		
	PCE_i vs B	**PCE_i vs D**	**D vs B**	**PCE_i (%)**	**B (%)**	**D (%/year)**
OPV	0.04	-0.08	0.31	6.2%	30%	6%
PVK	-0.46	0.20	0.26	16%	19%	9%

(Left) Pearson correlation coefficients of initial PCE (PCE_i), burn-in loss (B), and long-term degradation rate (D), and (Right) average device characteristics for OPV and PVK devices captured by the literature review.

2.2 Model development

The LCOE can be calculated by dividing the net present value (NPV) of the total costs incurred by the NPV of the total PV generation in the project lifetime:

$$LCOE = \frac{I_0 + \sum_{t=1}^{l} \frac{C_t}{(1+d)^t}}{\sum_{t=1}^{l} \frac{E_t}{(1+d)^t}} \qquad (1)$$

Here I_0 is the installation cost (USD); C_t are the total costs in year t (USD) comprising operating costs, and panel/inverter replacement costs at the end of their life; E_t is electricity generation in year t (kWh); l is the project life (years); and d is the discount rate (%).

The model input parameters can be grouped into information about the PV modules (e.g. panel replacement year, panel cost or burn-in), the PV project (e.g. project lifetime, inverter lifetime and land rental), and location (e.g. local discount rate, PV array tilt and peak solar hours per year). A list of input parameters for PV modules and the project, together with justifications for values chosen, can be found in Section 2.1 of Appendix A, whilst location information can be found in Section 2.2 of Appendix A. However, in summary, we selected a project location of Suva, Fiji due to its high yearly insolation and availability of underpinning data, though we stress that other arbitrary locations can be modelled using this approach. The project has 5.5 MWp installed initial capacity and is subject to a local discount rate of 10% over a lifetime of 20 years. These values are chosen to be typical of the location. Installation and balance of system costs scale with module efficiency to reflect changing land-use, cabling and infrastructure requirements for the project. From these data, costs are calculated using equations shown in Section 2.3 of Appendix A.

The electricity generation model accounts for changing PV capacity due to burn-in and following linear degradation as well as panel replacement. It is assumed that degradation only occurs during the hours of full sun in the project location, hence we defined the cumulative peak solar hours (S_c) from the installation date to inform calculations of PV capacity for a particular panel. Table A5 shows the monthly peak solar hours in the project location.

The time-dependence of PCE was parameterized to allow for calculation of PV capacity at any given time. We defined the following functions for B_F and D_F as the fractional loss in PCE as compared to the PCE at the start of the burn-in and linear degradation periods respectively, such that $PCE = PCE_i B_F$ during burn-in and $PCE = PCE_b D_F$ during linear degradation.

$$B_F(\%) = aS_c^{\ 2} + bS_c + 100 \qquad S_C \leq \tau_B \qquad (2)$$

$$D_F(\%) = d_L S_c + c + B \qquad S_C > \tau_B \qquad (3)$$

The variables d_L, a, b and c are calculated from burn-in (B) and linear degradation (D) values for the candidate PV modules as shown in Table A7. The coefficients a and b describe a quadratic burn-in period, while d_L and c are the slope and intercept of a linear degradation region. These equations lead to a time dependence of PCE of a form shown in Figure A1. Equation 2 and 3 were selected as they described the general form of emerging PV degradation behavior revealed in the literature review presented in section 2.1. However, we note that this framework could be modified to accept other arbitrary degradation functions. A feature within our model is the ability to replace panels at arbitrary points within the lifetime of the project, to reflect the possibility of supporting infrastructure having a lifetime longer than panels. We note that while panel replacement has been considered in previous LCOE models [9], the focus in that study was the potential cost advantage due to future improvements in tooling for emerging PV, here we use panel replacement to mitigate the impact of degradation. S_c resets to zero after panels are replaced at the end of each panel replacement year such that each new panel starts with the same PCE_i and degradation trajectory as the previous panel. Note that zero burn-in (B = 0%) can be accommodated within the model by setting τ_B =0, such that linear degradation begins immediately following installation.

The peak capacity of the PV array, P at any moment in time is thus represented as:

$$P = P_{arr} B_F \qquad S_C \leq \tau_B \qquad (4)$$

$$P = P_{arr} \frac{(100-B)}{100} D_F \qquad S_C > \tau_B \qquad (5)$$

Where P_{arr} is the size of PV array (Table A3) and B is the Burn-in degradation, %. Energy generation is calculated using the peak capacity at start of the project (P_{arr}), and the end of each month, *m* (P_m) according to equations (4) and (5). For ease of notation, we subsequently describe the initial size of the PV array P_{arr} as P_0. Electricity Generation in month *m* is thus calculated as follows:

$$E_m = Y_m \times \frac{P_m + P_{m-1}}{2} \qquad (6)$$

Where E_m = Electricity Generation at current month, Y_m = Yield at current month (from Table A5), and P_{m-1} = Peak capacity at previous month. Monthly electricity generation values are aggregated for each year of the project, and joined with yearly project costs, to calculate the LCOE using equation (1) for the 20-year project.

3. Results and Discussion

3.1 Impact of degradation on LCOE

We begin by discussing the impact of degradation in emerging PV devices, taking the impacts of burn-in (i.e. short time degradation) and following linear degradation separately as the two only show weak correlation. **Figure 2**A shows predicted LCOE for a PV panel having PCE_i = 10% as a function of D with panel replacement after every 2, 5 or 10 years compared to no replacement in the 20-year project. We note that at the time of writing, champion PV modules for OPVs and PVKs have efficiencies of 11.7% and 17.9% [65] respectively, hence our choice of 10% and 20% PCE_i in most calculations shown here represents values that might realistically be achieved in the field in the near future. Two cases of burn-in are considered, B = 10% and 40%, representing typical values within the spread reported in the literature, as discussed in section 2.1. 40% represents the most repeated B value in the upper end of literature, whilst 10% represents a B value in the lower end of literature. As may be anticipated, more frequent panel replacement reduces sensitivity of LCOE to D but increases project costs. For the project considered, this behavior results in substantial differences in the optimal panel replacement year as a function of degradation rate, D. We note that for the cases considered, the optimal panel replacement year does not match the 'stabilized lifetime' (T_{S80}), defined as the length of time taken for the post burn-in efficiency to drop by 20%. Optimal replacement years are additionally found to be independent of PCE_i and B for specific installations, as intersections between pairs of panel replacement curves (e.g. 20 years and 10 years at D = 3%) occurs for the D when the fractional differences in PV yield and project cost match. However, it is important to note that replacing panels too frequently may result difficult for the construction and installation sectors. Whilst emerging PV modules are expected to reduce embodied carbon dioxide in as compared to Si PV [66], one should also consider the impact of recyclability, disposal and use of critical elements used by these new technologies. Figure 2B shows predictions of LCOE as a function of burn-in loss, B between 5 and 40% for modules having PCE_i = 10% and four scenarios of D = 10, 4, 2 and 1 %/year. The values of B and D are chosen to represent the spread reported in the literature for emerging PV as shown in Figure 1. Panels replacement is chosen to occur after either 5 years, 10 years, or not at all during the 20-year project, according to the lowest LCOE for the value of D shown in Figure 2A. It is shown that predicted LCOE varies non-linearly with B, and that LCOE approaches a local minimum as B and D approach the lower end of the ranges considered. The non-linearity with B can be understood since LCOE emphasizes production and costs early in project life. Figure 2B also suggests that candidate materials and architectures may be selected based on a balance of good short-term and long-term degradation, rather than 'champion' status in either.

(A)

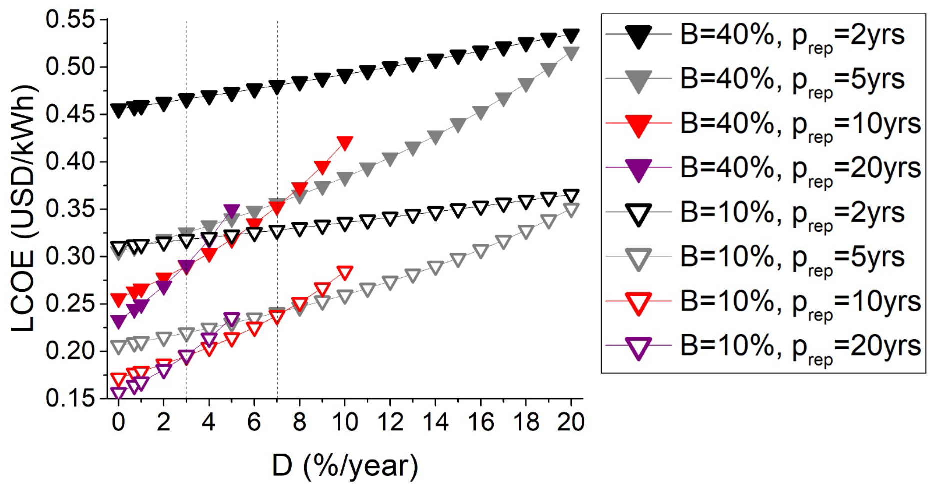

(B)

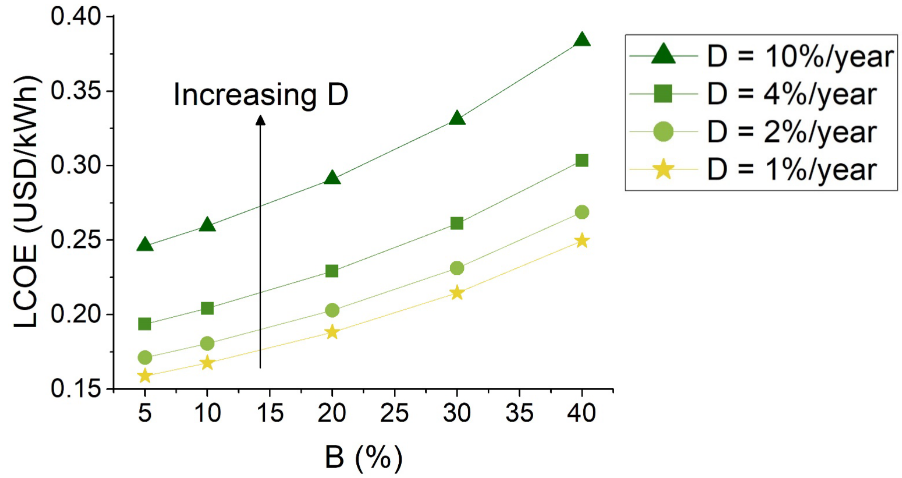

Figure 2. Impact of burn-in and degradation rate in LCOE

(A) Predictions of LCOE as a function of degradation rate, D for panel replacement years of 2 (black), 5 (grey), 10 (red) and no replacement within 20 year project (purple), with PCE_i = 10% and burn-in losses of 40% (solid) and 10% (open). (B) Predictions of LCOE as a function of burn-in, B for modules with PCE_i = 10% and D = 10%/year (up triangles), 4%/year (squares), 2%/year (circles) and 1%/year (stars). A module cost matching Si PV (0.245 USD/Wp) was considered in all cases.

3.2 Impact of module cost on LCOE

Having established the impact of the degradation profile on LCOE, our focus now shifts to the potential low module cost that is also characteristic of emerging PV. We highlight that there is a significant range of predicted module costs for emerging PV reported in the literature (Table A2). As such, our approach is not to define a specific module cost that is characteristic of a particular PV, rather it is to predict LCOE over a much wider range of module costs than predicted in the literature to account for uncertainty and future improvements. **Figure 3** shows predicted LCOE for emerging PV modules with PCE_i = 10%, B = 40% and D = 10%/year, 2%/year and 1%/year, representing values within the spread reported in the literature. These modules with a range of D are compared to those which instead have reduced burn-in (PCE_i = 10%, B = 10% and D = 10%/year) or increased initial efficiency (PCE_i = 20%, B = 40%, D = 10%/year). As before, modules with D = 10%/year are replaced every 5 years, and modules with D = 2 and 1%/year are not replaced within the 20-year project lifetime.

It is observed that LCOE varies approximately linearly with module cost above ~1 USD/Wp, but converges to a minimum value below ~0.2 USD/Wp due to the fixed costs of PV installation in the model such as site establishment, grid connection, etc. The minimum LCOE at low module cost varies substantially with PCE_i and B, but is relatively insensitive to D. Conversely, at high module cost, doubling PCE_i has less impact. These observations demonstrate that the present model can give directed advice as to the most effective routes to improve LCOE. For example, a device which offers a module cost below 0.2 USD/Wp may benefit from more expensive fluorinated encapsulation to improve degradation [67]. Conversely, if a PV technology has module

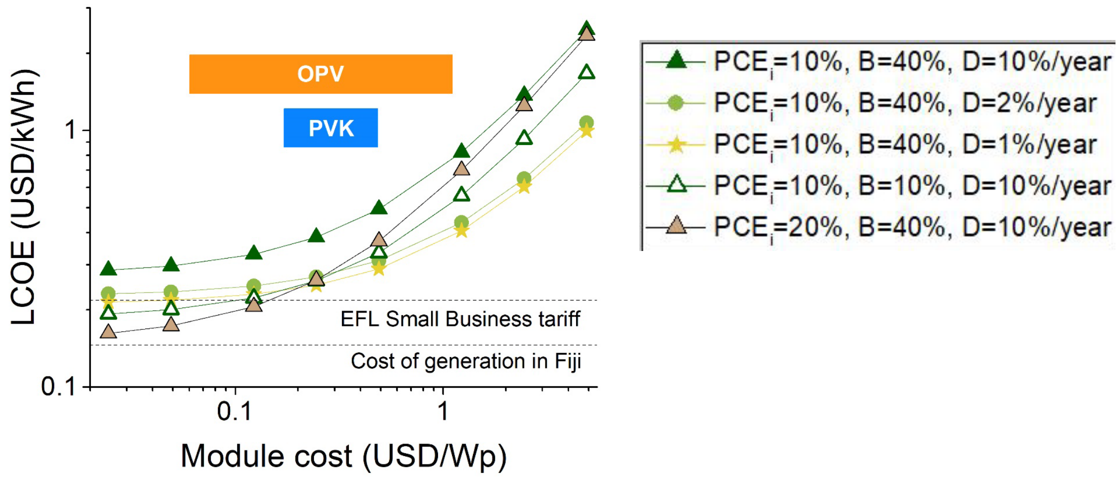

Figure 3. Impact of module cost in LCOE

Predictions of LCOE as a function of module cost for panels with PCE_i = 10% (shades of green) with burn-in B = 40% (closed) with D = 10%/year (triangles), 2%/year (circles) and 1%/year (stars). Compared to this are modules with PCE_i = 10%, B = 10% with D = 10% (green open triangles) and PCE_i = 20%, B = 40% with D = 10%/year (light brown triangles). Horizontal bars show range of predicted Module Costs for PVK and OPV.

costs exceeding 2 USD/Wp, reductions in the module cost, such as through manufacturing processes or lower cost materials, are predicted to have more substantial benefits than marginal improvements in PCE_i. We note that the dependence of LCOE on module cost varies significantly over the range of predicted values of module cost. These findings motivate further research in defining the expected costs of commercially manufactured emerging PV modules, as these will enable a more quantitative approach to optimizing LCOE. By contrast, reducing burn-in is always beneficial, as in this example, reducing burn-in from 40% to 10% reduces LCOE by

~32%. However, as observed in Figure 3, reducing B is recommended over reducing D when the module cost is low (<0.2 USD/Wp), and the contrary when the module cost is higher than 0.2 USD/Wp.

3.3 Inter-relationship between PV metrics and LCOE

Having examined the impact of degradation, module cost and initial efficiency in sections 3.1 and 3.2, we now taking a broader view of the inter-relationship between these parameters. **Figure 4**A-C are contour plots of LCOE predictions as pairwise functions of PCE_i, B and module cost over the range of values reported in the literature and allowing for possible future improvements. Here, a degradation rate of D = 10%/year and panel replacement every 5 years are assumed, although qualitatively similar data is shown in Appendix A Figure A4 for an assumed D = 2%/year with no panel replacement in the 20-year project. These data allow quantitative comparison of different technologies as a function of the PCE_i, B and module cost they offer. For example, a 7.5% PCE_i module with module cost of 0.12 USD/Wp provides an equivalent LCOE as a 25% PCE_i module with module cost of 0.75 USD/Wp. However, it is noted that despite the equivalence in LCOE, optimizing strategies would be different, since the LCOE of the 7.5% PCE_i module would not benefit significantly from further reductions in module cost, whilst the 25% PCE_i module would. More generally, Figure 4 show that the gradient of LCOE is a complex function of the lifetime energy yield, thus emphasizing the benefit of LCOE modelling to inform technology development.

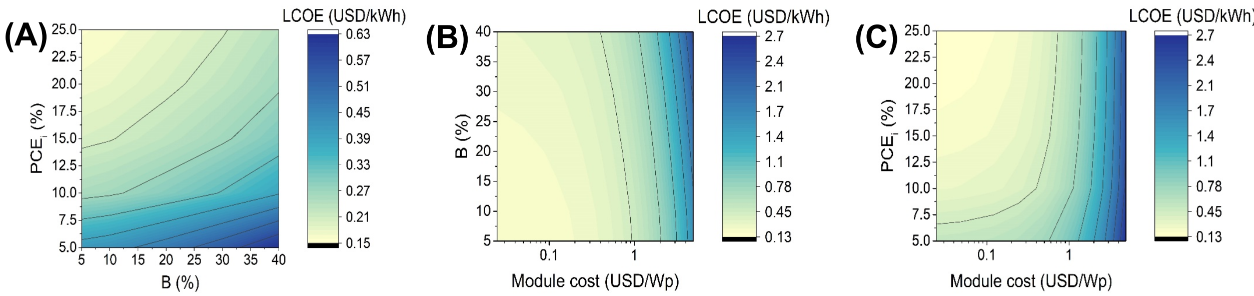

Figure 4. Inter-relationship between PV metrics and LCOE

Contour plots of predicted LCOE as a function of (A) PCE_i and burn-in, B assuming module cost 0.245 USD/Wp; (B) Module cost and burn-in, B assuming PCE_i = 10%; (C) PCE_i and module cost assuming burn-in, B = 40%. In all cases D is assumed = 10%/year with panel replacements every 5 years.

3.4 Contextualizing LCOE within the electricity market

Having predicted the LCOE for a wide range of emerging PV parameters, we dwell on the competitiveness of these values with respect to other forms of energy generation. LCOE must not only be compared between different solar PV types. It is important to consider how LCOE may compare to electricity generation or supply costs from traditional sources on the grid. Therefore, LCOE values corresponding to low and high scenarios of electricity generation and sale in Fiji are now considered. These values were calculated using similar parameters to the model (10% discount rate, 2.1% inflation and in this case a 25 years lifetime as a mature technology), based on the cost of generation from the Pacific Power Association report (0.1240 USD/kWh) [68] and the small business tariff of Energy Fiji Limited (EFL) (0.1849 USD/kWh) [69], which have an LCOE of 0.1461 USD/kWh and 0.2178 USD/kWh respectively. For context, electricity costs in Fiji are in general cheaper than in European countries (e.g. UK ~0.234-0.255 USD/kWh) [70], but not as cheap as in USA (~0.111-0.149 USD/kWh) [70] and other regions in America or Africa. However, we stress that the predicted LCOE values here are only applicable to Fiji, and that to comment on viability of emerging PV in other locations would require calculations with appropriate insolation and financial data for the location. It is observed in Figure 3 that most scenarios for emerging PV modules would require a module cost of less than 0.1 USD/Wp to compete with the reference values. However, Figure A3 in Appendix A shows that increasing PCE_i to 20% and 30%, as may be possible in high-performance single junction or tandem PVs [71], widens the range of module costs and degradation parameters for which emerging PV is competitive with reference sale values. For example, it is predicted that panels with B = 40% and D = 2% beat the cost of generation for module costs less than 0.12 USD/Wp when PCE_i = 20%, and for module costs less than 0.25 USD/Wp when PCE_i = 30%.

3.5 LCOE Assessment of state-of-the-art emerging PV devices

Having gained insight into how the *typical* evolution of PCE with time for emerging PV impacts LCOE, we now present predicted LCOE for *specific* state-of-the-art PVK and OPV devices revealed in our literature review described in section 2.1 and listed in Appendix A Table A8. Only devices which were tested under light-soaking conditions and some form of encapsulation or protective atmosphere (listed in Appendix A) were considered. Further, to limit the number of variables being considered, all OPV and PVK devices have a burn-in period τ_B that is equal to the average for that device type (Table A3). Once again, the assumed project was a 5.5 MWp PV installation in Fiji with a local discount rate of 10% and a 20-year project lifetime. It was assumed that the module cost is equal to silicon (0.245 USD/Wp) due to significant variation in the estimated module price for PVK and OPV devices, noting that this value falls within the range of estimated module prices (Table A2). For each device, the LCOE was calculated for panel replacements every 2, 5, 10 and 20 years, and the lowest LCOE predicted was recorded for that particular device.

Figure 5A shows that a wide distribution of LCOE values are predicted for both PVK and OPV devices. Whilst PVK devices provide better LCOE on average as compared to OPV, the distributions overlap. Overall, two OPV devices and eight sets of PVK devices have predicted LCOE values below the higher selling price of 0.22 USD/kWh in Fiji, with seven of the PVK devices also undercutting the lower electricity sale price of 0.15 USD/kWh. We note that these predictions of LCOE are based on the properties of cell level devices and the performance of an equivalent module would be expected to be worse. However, one may expect modules to improve over time, and at time of writing, certified record initial efficiencies for modules are ~5 years behind those of cells for both PVK and OPV devices [62, 65]. Figure 5B, C and D show the dependence of predicted LCOE on individual B, D and PCE_i respectively, whilst associated statistical data are shown in **Table 2**. These data confirm the earlier supposition that the lowest predicted LCOE for both PVK and OPV technologies are not necessarily those with the highest PCE_i, but those with a balance of good efficiency and low burn-in and degradation rates. For example, the second highest PCE_i for OPVs within the dataset was 9.8%, but this device was predicted to have an LCOE of 0.41 USD/kWh because of

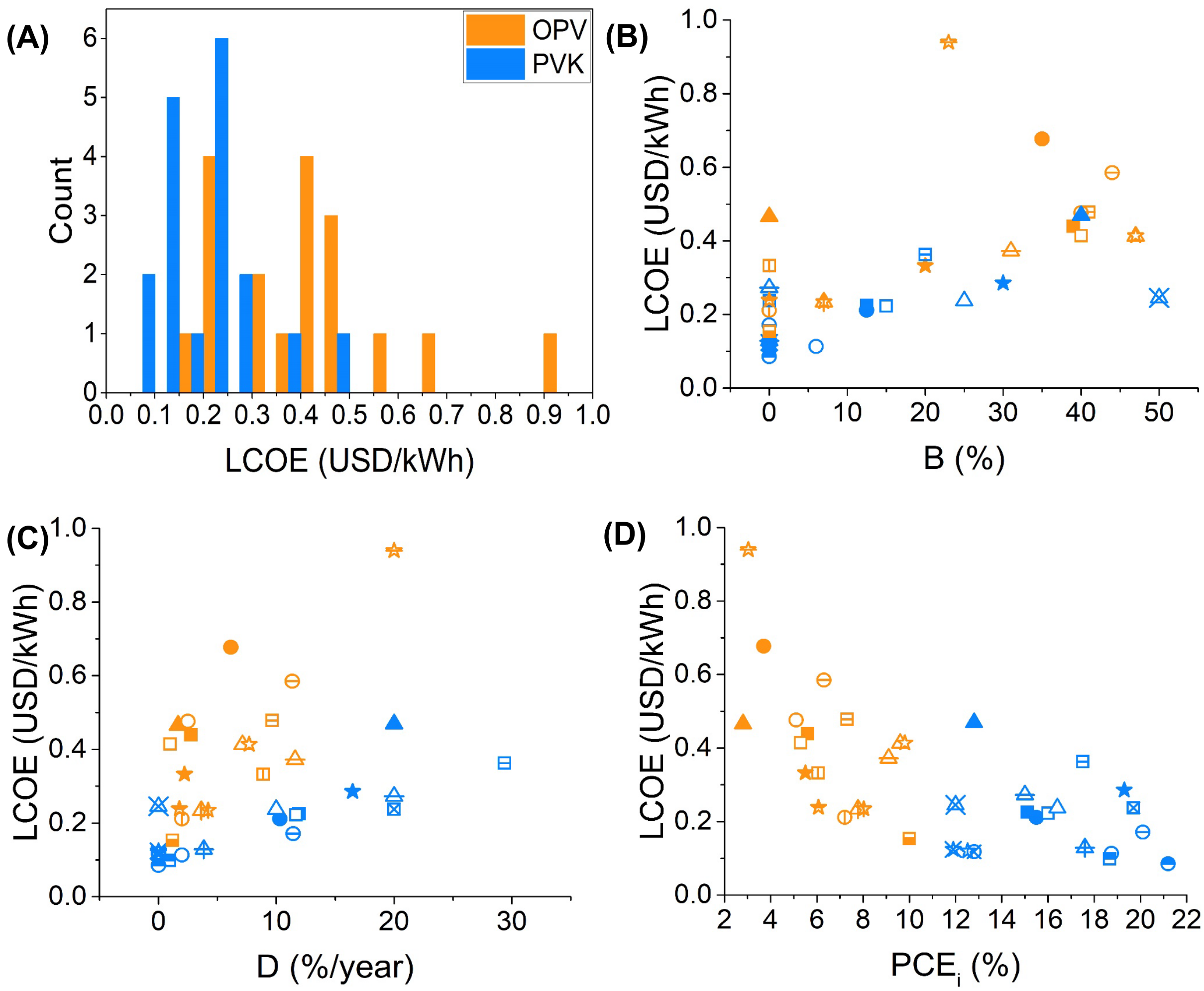

Figure 5. Predicted LCOE for *specific* state-of-the-art PVK and OPV devices

Predicted LCOE for PVK (blue) and OPV (orange) modules with parameters extracted from degradation measurements shown as (A) a histogram, and as a function of (B) B (C) D, and (D) PCE_i. Each symbol represents a unique device, the materials and architecture for which is listed in table A8 of the supplementary information.

high B and D, while an OPV with PCE_i of 7.2% was predicted to have a better LCOE of 0.21 USD/kWh as it had D = 2%/year degradation and minimal burn-in. While the finding that emerging PV devices with state-of-the-art initial efficiencies are not necessarily those with state-of-the-art LCOE, is not necessarily surprising, it nonetheless emphasizes the need to quantify energy yield over a devices' lifetime and to quantify LCOE if one is to have a sound basis for determining what technologies have potential for grid-scale applications.

Table 2. Statistical analysis of data displayed in Figure 5.

	Pearson coefficients			Average LCOE (USD/kWh)
	LCOE vs PCE_i	**LCOE vs D**	**LCOE vs B**	
OPV	-0.61	0.71	0.50	0.41
PVK	-0.19	0.82	0.70	0.21

Table 2 shows that there are significant differences between the correlation coefficients for PVK and OPV technologies, suggesting that optimal development strategies for emerging PVs may be different. We analyze this further in **Figure 6**A-B, in which we predict the LCOE for an average OPV or PVK device respectively (Table 1), which is then subsequently improved in a number of different ways. Specifically, we take the average device for OPVs or PVKs and either: reduce module cost by factor 2; reduce burn-in and degradation by factor 2; reduce burn in by factor 2; reduce degradation by factor 2; or increase PCE_i by factor 2. These predictions are compared against the champion LCOE values for OPVs or PVKs, and values corresponding for commercial Si PV (PCE_i = 20%, B = 2%, D = 0.7%/year). Again, we emphasize that the predictions for OPV and PVK are for cell-level devices, and so would not expect these LCOE values to be reflected in an OPV and PVK module at present. That said, we note that whilst the largest reduction in LCOE comes about for both OPV and PVK devices when PCE_i is doubled, in the case of the PVK, the effectiveness of doubling efficiency is similar to that of halving burn-in and degradation. These data may therefore indicate that PVK devices are reaching an inflection point, where the focus of future optimization may more fruitfully be expended on reducing degradation than improving efficiency. Supporting this conjecture is the observation that the champion PVK LCOE prediction is for a device with zero burn-in and degradation. We note that the prediction for this champion cell-level PVK device is lower than that for a Silicon PV module, perhaps indicating that cost-competitive PVK modules may be a viable prospect in the future.

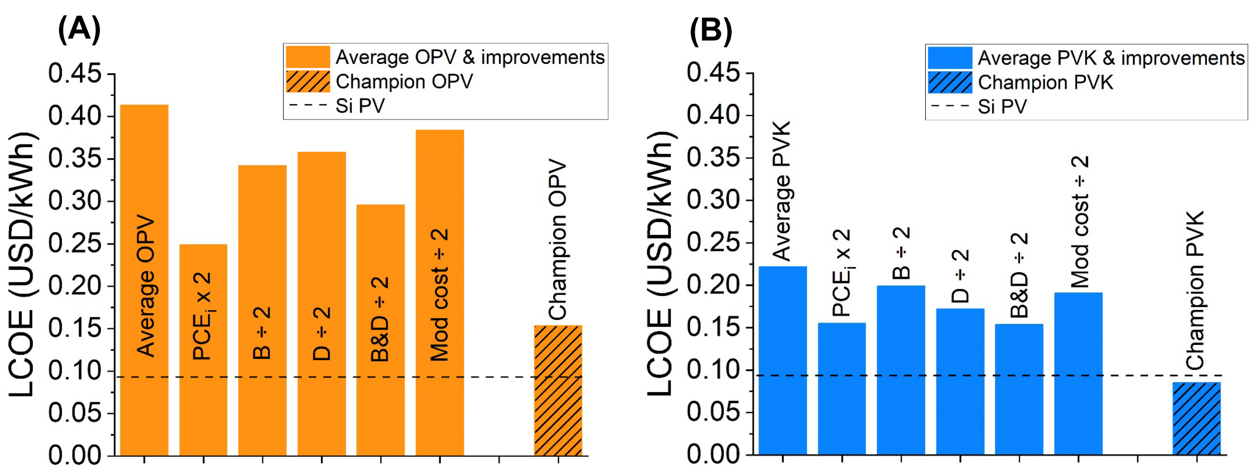

Figure 6. Average and Champion OPV & PVK vs Si PV LCOE

Comparison of literature review (A) Average OPV (PCE_i=6.2%, B=30%, D=6%/year) with improvements, Champion OPV (PCE_i=10%, B=0%, D=1.18%/year), and (B) Average PVK (PCE_i=16%, B=19%, D=9%/year) with improvements & Champion PVK (PCE_i=21.2%, B=0%, D=0%/year) vs a Si PV baseline (PCE_i=20%, B=2%, D=0.7%/year). Module cost assumed to be 0.245 USD/Wp for all, except when Mod cost ÷ 2 is indicated (0.1225 USD/Wp).

Optimal development strategies were explored further by calculating numerically the partial derivatives of LCOE with respect to module cost, PCEi, B and D at the point corresponding to each individual device. These data are displayed as box plots in

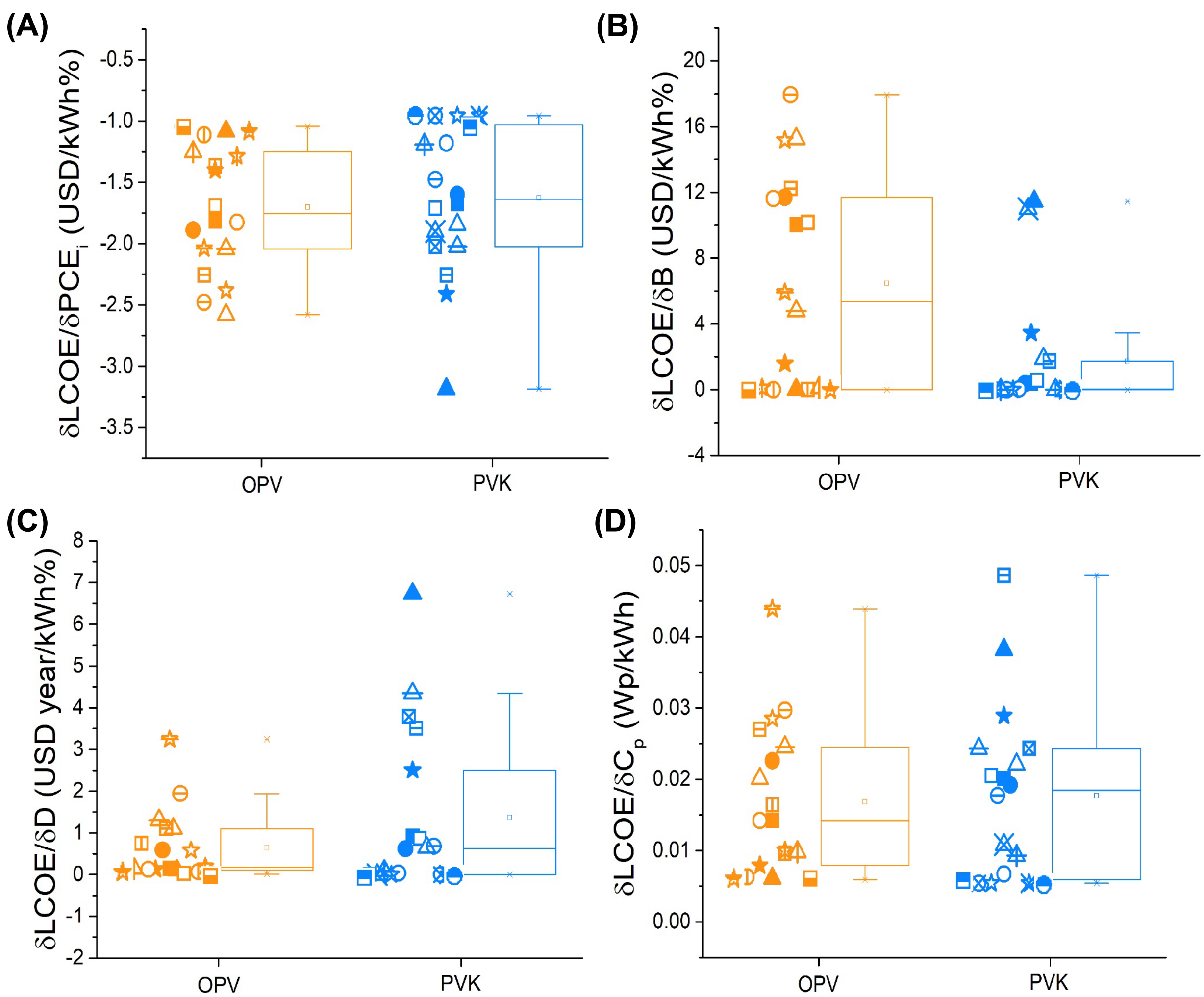

Figure 7. Partial derivatives of LCOE vs Emerging PV parameters

Statistical data for partial derivatives of LCOE with respect to (A) PCEi, (B) B, (C) D and (D) C_p for OPV (orange) and PVK (blue) light-soaked devices. Each symbol represents a unique device, the materials and architecture for which is listed in table A8 of the supplementary information.

Figure 7 and as pair-wise scatter plots in Figure A5 of Appendix A. It is apparent that the partial derivatives vary significantly both between and within populations of PVK and OPV devices. This is a key result, as it shows that one must consider the lifetime energy yield of an individual PV architecture (quantified by PCE_i, B and D) if one is to make quantitative recommendations on how LCOE is best optimized. Relating to this result, it is notable that while papers reporting lifetime energy yield (e.g. ISOS [63, 64] L or O standards) are increasing in number, they are significantly outnumbered by those which focus upon initial performance. Hence to realize the full benefits of an LCOE approach to select and optimize emerging PV devices, the focus of device studies must find a new balance that encompasses the initial performance, degradation, and cost.

4. Conclusions

This paper presents and utilizes a time-resolved model of LCOE which captures both the degradation behavior of emerging PV and realistic PV installation design and costing. The degradation model is informed by a systematic review of state-of-the-art Perovskite and Organic PV devices, which in turn is used as an input dataset to assess LCOE potential of these materials and architectures. The optimal route to optimize LCOE is shown to depend critically upon the present module cost, initial efficiency, and following degradation offered by a technology. This, coupled with the substantial variation in lifetime performance of emerging PV, means that optimal strategies to improve LCOE are specific to individual active layer compositions. In particular, our findings demonstrate that the prevailing focus on efficiency of new panels is not a useful measure of technology feasibility, as for example panels with a low efficiency and low degradation (PCE_i=10%, B=10%, D=1%/year) result in a better LCOE than panels with a high efficiency and high degradation (PCE_i=20%, B=40%, D=10%/year) in the 5 MWp Fiji scenario here analyzed (0.17 vs 0.26 USD/kWh). Notwithstanding this challenge, the data suggest that if modules can achieve the same characteristics as some of the cell level OPV and PVK devices examined here, emerging PV can compete on wholesale electricity markets. The framework presented here will also help ascertain how emerging PV technologies may prove economically viable in different markets and applications, as well as support researchers in this field who can often be distant from commercial pressures. For example, measures which can affect fixed costs, such as rooftop installation, printing on materials, encapsulation in panes, low light performance, and so on, can be evaluated using an LCOE approach. As such, an LCOE modelling approach influences not only technology choice, but also the direction of research to applications for that technology, extending beyond the wholesale market approach considered here.

Acknowledgements

The authors acknowledge support from EPSRC, UK (North East Centre for Energy Materials EP/R021503/1) and CONACyT-SENER for the award of a scholarship (BAND) (625176). The authors also thank Dr B. Mendis and Dr D. Halliday (Department of Physics, Durham University, UK) for internal peer review of the manuscript and helpful suggestions.

Author contributions

BAND contributed to investigation, validation, visualization, writing (original draft). AFC contributed to software development and validation. CG contributed to conceptualization, writing (original draft), supervision. All authors contributed to methodology, formal analysis and writing (review and editing).

Declaration of interests

The authors declare no completing interests.

References

[1] Chang NL, Ho-Baillie AWY, Vak D, Gao M, Green MA, Egan RJ. Manufacturing cost and market potential analysis of demonstrated roll-to-roll perovskite photovoltaic cell processes. Sol Ener Mat and Sol C. 2018;174:314-24.
[2] Li N, McCulloch I, Brabec CJ. Analyzing the efficiency, stability and cost potential for fullerene-free organic photovoltaics in one figure of merit. Ener Environ Sci. 2018;11:1355-61.
[3] Jordan DC, Kurtz SR. Photovoltaic Degradation Rates-an Analytical Review. Progr Photo: Res App. 2013;21:12-29.
[4] Guo J, Min J. A Cost Analysis of Fully Solution-Processed ITO-Free Organic Solar Modules. Adv Ener Mat. 2019;9.
[5] Li Z, Zhao Y, Wang X, Sun Y, Zhao Z, Li Y, et al. Cost Analysis of Perovskite Tandem Photovoltaics. Jou. 2018;2:1559-72.
[6] Song Z, McElvany CL, Phillips AB, Celik I, Krantz PW, Watthage SC, et al. A technoeconomic analysis of perovskite solar module manufacturing with low-cost materials and techniques. Ener Environ Sci. 2017;10:1297-305.
[7] Gambhir A, Sandwell P, Nelson J. The future costs of OPV – A bottom-up model of material and manufacturing costs with uncertainty analysis. Sol Ener Mat and Sol C. 2016;156:49-58.
[8] Tran TTD, Smith AD. Incorporating performance-based global sensitivity and uncertainty analysis into LCOE calculations for emerging renewable energy technologies. Appl Ener. 2018;216:157-71.
[9] Jean J, Woodhouse M, Bulović V. Accelerating Photovoltaic Market Entry with Module Replacement. Jou. 2019;3:2824-41.
[10] Jordan DC, Kurtz SR, VanSant K, Newmiller J. Compendium of photovoltaic degradation rates. Progr Photo: Res App. 2016;24:978-89.
[11] Mulligan CJ, Bilen C, Zhou X, Belcher WJ, Dastoor PC. Levelised cost of electricity for organic photovoltaics. Sol Ener Mat and Sol C. 2015;133:26-31.

[12] Bovill E, Scarratt N, Griffin J, Yi H, Iraqi A, Buckley AR, et al. The role of the hole-extraction layer in determining the operational stability of a polycarbazole:fullerene bulk-heterojunction photovoltaic device. Appl Phys Lett. 2015;106.
[13] Cheacharoen R, Mateker WR, Zhang Q, Kan B, Sarkisian D, Liu X, et al. Assessing the stability of high performance solution processed small molecule solar cells. Sol Ener Mat and Sol C. 2017;161:368-76.
[14] Du X, Heumueller T, Gruber W, Classen A, Unruh T, Li N, et al. Efficient Polymer Solar Cells Based on Non-fullerene Acceptors with Potential Device Lifetime Approaching 10 Years. Jou. 2019;3:215-26.
[15] Gasparini N, Salvador M, Strohm S, Heumueller T, Levchuk I, Wadsworth A, et al. Burn-in Free Nonfullerene-Based Organic Solar Cells. Adv Ener Mat. 2017;7.
[16] Heumueller T, Mateker WR, Sachs-Quintana IT, Vandewal K, Bartelt JA, Burke TM, et al. Reducing burn-in voltage loss in polymer solar cells by increasing the polymer crystallinity. Ener Environ Sci. 2014;7:2974-80.
[17] Karpinski A, Berson S, Terrisse H, Mancini-Le Granvalet M, Guillerez S, Brohan L, et al. Anatase colloidal solutions suitable for inkjet printing: Enhancing lifetime of hybrid organic solar cells. Sol Ener Mat and Sol C. 2013;116:27-33.
[18] Kong J, Song S, Yoo M, Lee GY, Kwon O, Park JK, et al. Long-term stable polymer solar cells with significantly reduced burn-in loss. Nat Comm. 2014;5:5688.
[19] Mateker WR, Sachs-Quintana IT, Burkhard GF, Cheacharoen R, McGehee MD. Minimal Long-Term Intrinsic Degradation Observed in a Polymer Solar Cell Illuminated in an Oxygen-Free Environment. Chem Mat. 2015;27:404-7.
[20] Oh H, Sim HB, Han SH, Kwon YJ, Park JH, Kim MH, et al. Reducing Burn-In Loss of Organic Photovoltaics by a Robust Electron-Transporting Layer. Adv Mat Int. 2019;6.
[21] Pearson AJ, Hopkinson PE, Couderc E, Domanski K, Abdi-Jalebi M, Greenham NC. Critical light instability in CB/DIO processed PBDTTT-EFT:PC 71 BM organic photovoltaic devices. Org Electr. 2016;30:225-36.
[22] Roesch R, Eberhardt K-R, Engmann S, Gobsch G, Hoppe H. Polymer solar cells with enhanced lifetime by improved electrode stability and sealing. Sol Ener Mat and Sol C. 2013;117:59-66.
[23] Sapkota SB, Spies A, Zimmermann B, Dürr I, Würfel U. Promising long-term stability of encapsulated ITO-free bulk-heterojunction organic solar cells under different aging conditions. Sol Ener Mat and Sol C. 2014;130:144-50.
[24] Sung Y-M, Huang Y-C, Chien FS-S, Tsao C-S. Mechanism and Analysis of Thermal Burn-In Degradation of OPVs Induced by Evaporated HTL. IEEE Journ Photo. 2019;9:694-9.
[25] Voroshazi E, Cardinaletti I, Conard T, Rand BP. Light-Induced Degradation of Polymer:Fullerene Photovoltaic Devices: An Intrinsic or Material-Dependent Failure Mechanism? Adv Ener Mat. 2014;4.
[26] Yang X-Y, Niu M-S, Qin C, Bi P-Q, Chen Z-H, Feng L, et al. Unraveling the unstable amorphous phase evolution effect on burn-in loss in polymer-fullerene solar cells. Org Electr. 2019;71:156-63.
[27] Zhang Y, Bovill E, Kingsley J, Buckley AR, Yi H, Iraqi A, et al. PCDTBT based solar cells: one year of operation under real-world conditions. Sci Rep. 2016;6:21632.
[28] Zhang Y, Yi H, Iraqi A, Kingsley J, Buckley A, Wang T, et al. Comparative indoor and outdoor stability measurements of polymer based solar cells. Sci Rep. 2017;7:1305.
[29] Al-Ahmad AY, Almayhi F, Al-Mudhaffer MF, Griffith MJ, Liu W, Li S, et al. A nuanced approach for assessing OPV materials for large scale applications. Sustainable Energy & Fuels. 2020;4:940-9.
[30] Greenbank W, Djeddaoui N, Destouesse E, Lamminaho J, Prete M, Boukezzi L, et al. Degradation Behavior of Scalable Nonfullerene Organic Solar Cells Assessed by Outdoor and Indoor ISOS Stability Protocols. Energy Technology. 2020.
[31] Jiang Z, Wang F, Fukuda K, Karki A, Huang W, Yu K, et al. Highly efficient organic photovoltaics with enhanced stability through the formation of doping-induced stable interfaces. Proc Natl Acad Sci U S A. 2020;117:6391-7.

[32] Burlingame Q, Huang X, Liu X, Jeong C, Coburn C, Forrest SR. Intrinsically stable organic solar cells under high-intensity illumination. Nat. 2019;573:394-7.
[33] Xu X, Xiao J, Zhang G, Wei L, Jiao X, Yip H-L, et al. Interface-enhanced organic solar cells with extrapolated T80 lifetimes of over 20 years. Science Bulletin. 2020;65:208-16.
[34] Bracher C, Freestone BG, Mohamad DK, Smith JA, Lidzey DG. Degradation of inverted architecture CH3NH3PbI3-xClx perovskite solar cells due to trapped moisture. Ener Sci Eng. 2018;6:35-46.
[35] Chen W, Wu Y, Yue Y, Liu J, Zhang W, Yang X, et al. Efficient and stable large-area perovskite solar cells with inorganic charge extraction layers. Sci. 2015;350:944-8.
[36] Lee JW, Dai Z, Han TH, Choi C, Chang SY, Lee SJ, et al. 2D perovskite stabilized phase-pure formamidinium perovskite solar cells. Nat Comm. 2018;9:3021.
[37] Liang C, Zhao D, Li P, Wu B, Gu H, Zhang J, et al. Simultaneously boost diffusion length and stability of perovskite for high performance solar cells. Nano Ener. 2019;59:721-9.
[38] Roose B, Johansen CM, Dupraz K, Jaouen T, Aebi P, Steiner U, et al. A Ga-doped SnO2 mesoporous contact for UV stable highly efficient perovskite solar cells. Journ Mat Chem A. 2018;6:1850-7.
[39] Tan H, Jain A, Voznyy O, Lan X, Garcia de Arquer FP, Fan JZ, et al. Efficient and stable solution-processed planar perovskite solar cells via contact passivation. Sci. 2017;355:722-6.
[40] Tsai H, Nie W, Blancon JC, Stoumpos CC, Asadpour R, Harutyunyan B, et al. High-efficiency two-dimensional Ruddlesden-Popper perovskite solar cells. Nat. 2016;536:312-6.
[41] Turren-Cruz S-H, Hagfeldt A, Saliba M. Methylammonium-free, high-performance, and stable perovskite solar cells on a planar architecture. Sci. 2018;362:449-53.
[42] Wang Z, Lin Q, Chmiel FP, Sakai N, Herz LM, Snaith HJ. Efficient ambient-air-stable solar cells with 2D–3D heterostructured butylammonium-caesium-formamidinium lead halide perovskites. Nat Ener. 2017;2.
[43] Wang Z, McMeekin DP, Sakai N, van Reenen S, Wojciechowski K, Patel JB, et al. Efficient and Air-Stable Mixed-Cation Lead Mixed-Halide Perovskite Solar Cells with n-Doped Organic Electron Extraction Layers. Adv Mat. 2017;29.
[44] Wong-Stringer M, Game OS, Smith JA, Routledge TJ, Alqurashy BA, Freestone BG, et al. High-Performance Multilayer Encapsulation for Perovskite Photovoltaics. Adv Ener Mat. 2018;8.
[45] Xie J, Arivazhagan V, Xiao K, Yan K, Yang Z, Qiang Y, et al. A ternary organic electron transport layer for efficient and photostable perovskite solar cells under full spectrum illumination. Journ Mat Chem A. 2018;6:5566-73.
[46] Lv Y, Zhang H, Liu R, Sun Y, Huang W. Composite Encapsulation Enabled Superior Comprehensive Stability of Perovskite Solar Cells. ACS Appl Mater Interfaces. 2020;12:27277-85.
[47] Tumen-Ulzii G, Qin C, Klotz D, Leyden MR, Wang P, Auffray M, et al. Detrimental Effect of Unreacted PbI2 on the Long-Term Stability of Perovskite Solar Cells. Adv Mat. 2020;32:e1905035.
[48] Mei A, Li X, Liu L, Ku Z, Liu T, Rong Y, et al. A hole-conductor-free, fully printable mesoscopic perovskite solar cell with high stability. Sci. 2014;345:295-8.
[49] Bella F, Griffini G, Correa-Baena J, Saracco G, Gratzel M, Hagfeldt A, et al. Improving efficiency and stability of perovskite solar cells with photocurable fluoropolymers. Sci. 2016;354:203-6.
[50] Zheng X, Hou Y, Bao C, Yin J, Yuan F, Huang Z, et al. Managing grains and interfaces via ligand anchoring enables 22.3%-efficiency inverted perovskite solar cells. Nat Ener. 2020;5:131-40.
[51] Grancini G, Roldan-Carmona C, Zimmermann I, Mosconi E, Lee X, Martineau D, et al. One-Year stable perovskite solar cells by 2D/3D interface engineering. Nat Comm. 2017;8:15684.
[52] Leijtens T, Eperon GE, Pathak S, Abate A, Lee MM, Snaith HJ. Overcoming ultraviolet light instability of sensitized TiO(2) with meso-superstructured organometal tri-halide perovskite solar cells. Nat Comm. 2013;4:2885.
[53] Mateker WR, McGehee MD. Progress in Understanding Degradation Mechanisms and Improving Stability in Organic Photovoltaics. Adv Mat. 2017;29.

[54] Li Z, Wu F, Lv H, Yang D, Chen Z, Zhao X, et al. Side-Chain Engineering for Enhancing the Thermal Stability of Polymer Solar Cells. Adv Mat. 2015;27:6999-7003.
[55] Baran D, Gasparini N, Wadsworth A, Tan CH, Wehbe N, Song X, et al. Robust nonfullerene solar cells approaching unity external quantum efficiency enabled by suppression of geminate recombination. Nat Comm. 2018;9:2059.
[56] Saliba M, Stolterfoht M, Wolff CM, Neher D, Abate A. Measuring Aging Stability of Perovskite Solar Cells. Jou. 2018;2:1019-24.
[57] ArcGIS Web Application, 2020. https://power.larc.nasa.gov/data-access-viewer/ (Accessed 01-Feb Feb 2020).
[58] Zhang Y, Samuel IDW, Wang T, Lidzey DG. Current Status of Outdoor Lifetime Testing of Organic Photovoltaics. Adv Sci. 2018;5:1800434.
[59] Grätzel M. The Rise of Highly Efficient and Stable Perovskite Solar Cells. Accounts of Chemical Research. 2017;50:487-91.
[60] Bi E, Tang W, Chen H, Wang Y, Barbaud J, Wu T, et al. Efficient Perovskite Solar Cell Modules with High Stability Enabled by Iodide Diffusion Barriers. Joule. 2019;3:2748-60.
[61] Wang J, Zhang J, Zhou Y, Liu H, Xue Q, Li X, et al. Highly efficient all-inorganic perovskite solar cells with suppressed non-radiative recombination by a Lewis base. Nat Commun. 2020;11:177.
[62] NREL Best Research-Cell Efficiency Chart, 2020. https://www.nrel.gov/pv/cell-efficiency.html (Accessed 09-Jun 2020).
[63] Khenkin MV, Katz EA, Abate A, Bardizza G, Berry JJ, Brabec C, et al. Consensus statement for stability assessment and reporting for perovskite photovoltaics based on ISOS procedures. Nature Energy. 2020;5:35-49.
[64] Reese MO, Gevorgyan SA, Jørgensen M, Bundgaard E, Kurtz SR, Ginley DS, et al. Consensus stability testing protocols for organic photovoltaic materials and devices. Solar Energy Materials and Solar Cells. 2011;95:1253-67.
[65] NREL Champion Photovoltaic Module Efficiency Chart, 2020. https://www.nrel.gov/pv/module-efficiency.html (Accessed 09-Jun 2020).
[66] Tian X, Stranks SD, You F. Life cycle energy use and environmental implications of high-performance perovskite tandem solar cells. Sci Adv. 2020;6:1-10.
[67] Uddin A, Upama M, Yi H, Duan L. Encapsulation of Organic and Perovskite Solar Cells: A Review. Coat. 2019;9.
[68] PPA Benchmarking Report, 2018. https://www.ppa.org.fj/wp-content/uploads/2019/09/2018-FY-Benchmarking-Report_update_220719-FINAL.pdf (Accessed 05-May 2020).
[69] Energy Fiji Limited Small Business Tariffs, 2019. http://efl.com.fj/your-business/electricity-tariffs-and-rates/small-business-tariffs/ (Accessed 05-May 2020).
[70] Global Electricity Prices, 2020. https://www.globalpetrolprices.com/electricity_prices/ (Accessed 19-Jan 2021).
[71] Oxford PV hits new world record solar cell, 2020. https://www.oxfordpv.com/news/oxford-pv-hits-new-world-record-solar-cell (Accessed 15-Jan 2021).